

A simplified method to calculate atmospheric CO₂ equivalency for changing surface albedo

Hashem Akbari¹

Heat Island Group, Concordia University, Montreal, Canada

ABSTRACT

Urban surfaces (roofs, pavements) with high solar reflectance (albedo) reduce solar energy absorbed by buildings and pavements, leading to a reduction in air-conditioning use and improved indoor thermal condition in non-conditioned buildings. In addition, cool surfaces improve summertime outdoor environment that in turn yield a better urban air quality, reduce morbidity and mortality. A reduction in cooling energy use reduces demand for electricity generation and lowers CO₂ emissions from fossil fuel power plants. Independent of the direct CO₂ reduction, high-albedo urban surfaces reflect a greater fraction of solar shortwave radiation back to space and create a negative radiative forcing (RF) that counters the RF induced by accumulation of greenhouse gases (primarily CO₂) in the atmosphere. Previously, a method based on equating the RF on top of the atmosphere (TOA) was introduced to calculate a *global-averaged* CO₂ equivalency offset for increasing albedo of urban surfaces. Here, a simplified technique is introduced to calculate a *regional* CO₂-equivalency of changes on albedo of land surfaces. The required input for this technique is the regional global horizontal insolation (GHI) on TOA and ground surface. Using this simplified model, calculations are carried out for about 4400 weather stations world-wide. These calculations showed that the world-wide median CO₂ offset was about 2 kg per 0.01 albedo change of a m² of a surface. The CO₂ offset is highest where the atmospheric transmittance is high. The CO₂ offset is about 2-3 kg around the equator, 1.5 - 4 kg for -30° to -20° latitude and 1 - 5 kg for 20° to 30° latitude, depending on local cloud cover. This method would allow development of country-specific policies to monetize the effect of high-albedo urban surfaces to counter global warming and climate change.

Keywords: High albedo surfaces, CO₂ offset, Urban Heat Island

Introduction

Urban surfaces (roofs and pavements) with high solar reflectance (hereafter referred as cool surfaces) absorb less of incoming shortwave solar radiation and stay cooler under the sun. A cool roof conducts less heat into the building resulting in less air-conditioning energy use in conditioned buildings and improves comfort in non-conditioned buildings (Akbari et al., 1999). In some commercial buildings, application of a cool roof may result in downsizing of the air conditioner and air handler systems that run more efficiently during the partial-load conditions and even save electricity during heating season by using less electricity for air-handling systems (Hosseini and Akbari, 2016).

Cool roofs and cool pavements (together an independently) alter the surface heat balance at a community which can result in a lower summer time ambient temperature and reduce urban heat island. Lower summertime ambient temperatures typically result in a better

¹ Corresponding author email: Hashem.Akbari@Concordia.ca

ambient air quality (lower concentration of pollutants), improved pedestrian comfort, and lower morbidity and mortality during heat storms (Jandaghian and Akbari, 2021).

Cool roofs and pavements also reflect a significant fraction of incoming shortwave solar radiation that escape the Earth's atmosphere helping to counter global warming. This aspect of reflective surfaces is referred to as a geoeengineering technology. Scientists have been studying geoeengineering technologies as methods to rapidly respond to extreme climate change (Vaughan and Lenton, 2011). These technologies, naming a few, include: increasing reflectance of large surfaces on the earth, increasing the atmospheric reflectance by injecting reflective particles in the atmosphere, and sequestering CO₂ from the atmosphere.

Increasing reflectance of the atmosphere and large land areas are experiments that their consequences are not fully understood. In contrast, humans have a long history of living in areas with white buildings and white cities throughout many parts of the world—cool cities.

Reducing atmospheric CO₂ concentration and increasing earth's albedo both cause a negative radiative forcing (RF) that result in slowing the rate of global warming. By equating the RF of incremental CO₂ emissions and increasing surface albedo, Akbari et al (2009) conducted a study to calculate a *global* equivalency between increasing reflectance of urban surfaces and reducing CO₂ emissions. They reported that reducing CO₂ emission by about 2.5 kg has the same effect on slowing the global warming as increasing albedo of 1 m² of a surface by 0.01. Akbari et al. (2012) further expanded this analysis by conducting simulations of the changes in the earth atmosphere temperature by increasing surface albedo and CO₂ emissions abatement. They reported that increasing the albedo of 1m² of a surface by 0.01 would have the same effect on long-term atmospheric temperature as reducing CO₂ emissions by 7 kg. The Intergovernmental Panel for Climate Change (IPCC) in their 5th assessment report adopted this 7 kg CO₂ offset for increasing surface albedo (IPCC 2014). Both studies reported only the world-wide effects; regional effects were not evaluated.

The RF from increasing surface albedo is expected to be most effective in regions with high insolation and less clouds. Here, we develop a method to calculate the incoming solar radiation on top of the atmosphere (TOA) for a given location. Then using locally available global horizontal insolation (GHI), we calculate the local atmospheric transmittance and top of the atmosphere RF by increasing a surface albedo. We equate this RF of albedo change with RF from CO₂ emissions to develop a *regional* equivalency between surface albedo change and CO₂ emission reduction. We carry out calculations for about 4400 stations around the world. The results are grouped together and presented by countries. The method can be used to develop a CO₂ equivalency (offset) and surface albedo change for a given location.

Methodology

To estimate the CO₂ offset by increasing surface albedo, we use a net zero energy balance of Radiative Forcing (RF) on top of the atmosphere (TOA),

$$dRF_{albedo\ of\ Earth} + dRF_{CO_2} = 0 \quad (1)$$

The albedo RF is estimated by

$$dRF_{albedo\ of\ Earth} = I da_{surface} f/A \quad (2)$$

Where, dRF_{albedo} = TOA change in RF, Wm⁻²; I = Global Horizontal Insolation (direct and diffuse), Wm⁻²; $da_{surface}$ = Change in albedo for a m² of a surface; f = Atmospheric transmission of reflected solar radiation; A = Earth surface area, 510.1x10¹² m².

For CO₂ RF, we use Mhyer et al (1998) equation

$$RF_{CO_2} = 5.35 \ln(C/C_0) \quad (3)$$

Where, RF_{CO_2} = CO₂ induced RF, Wm⁻²; C = Atmospheric CO₂ concentration; C_0 = Reference atmospheric CO₂ concentration.

The incremental change in RF is calculated by

$$dRF_{CO_2} = 5.35 dC/C \quad (4)$$

The current atmospheric CO₂ concentration is 421 ppm (NOAA 2022). Each ppm of atmospheric CO₂ concentration is about 7.821x10¹² kg of CO₂. Hence, the total atmospheric CO₂ content is about 3.293x10¹⁵ kg.

Substituting (2) and (4) in (1),

$$I(f) \frac{da_{surface}}{A} + 5.35 \frac{dC}{C} = 0 \quad (5)$$

Or,

$$dC/da_{surface} = -fIC/5.35A \quad (6)$$

Substituting the values of C and A, we get

$$dC/da_{surface} = -1.21 f I, \text{ kg/unit change of a m}^2 \text{ of surface albedo} \quad (7)$$

This equivalency can be represented per 0.01 change in the surface albedo as

$$dC/da_{surface} = -1.21 \times 10^{-2} f I, \text{ kg/0.01 change of a m}^2 \text{ of surface albedo} \quad (8)$$

Eq 8 can be used on an hourly basis to estimate the CO₂ offset for change in surface albedo. The total horizontal solar radiation, *I*, is a function of the time of the day, day of the year and seasonal climate conditions. Hence, the calculated hourly CO₂ equivalency (CO₂ offset) can vary significantly throughout hours of the year. A more stable CO₂ offset can be calculated by using the hourly values averaged for the year, i.e.

$$(dC/da_{surface})_{avg} = -1.21 \times 10^{-2} \sum_{i=1}^{8760} I_i f_i / 8670 \quad (9)$$

It is estimated that *dC* (change in CO₂ atmospheric concentration) is only a fraction *g* (~0.5) of the emitted CO₂, *C_{emitted}*. Hence, Eq 9 is scaled to show the emitted-CO₂ offset

$$(dC_{emitted}/da_{surface})_{avg} = \frac{-1.21 \times 10^{-2}}{g} \sum_{i=1}^{8760} f_i I_i / 8670 \quad (10)$$

Equation 10 is further simplified to

$$(dC_{emitted}/da_{surface})_{avg} = \frac{-1.21 \times 10^{-2}}{g} f_{avg} I_{avg} \quad (11)$$

Or, in the simplest form with *g* = 0.5 and *f_{avg}* from Eq 13,

$$(dC_{emitted}/da_{surface})_{avg} = -2.42 \times 10^{-2} I_{avg}^2 / I_{TOA} \quad (12)$$

In Eq 8, measured values of *I* is usually available for many weather stations around the globe. The atmospheric solar scattering and attenuation can be calculated by dividing *I* to the calculated TOA incoming solar radiation intensity (*I_{TOA}*),

$$f_{avg} = I_{avg} / I_{TOA} \quad (13)$$

The extraterrestrial solar radiation on a horizontal surface for a given hour of the day. *I_{TOA,I}*, is calculated by Eq 12

$$I_{TOA,i} = I_0 (1 + 0.033 \cos(\frac{360n}{365})) (\cos\varphi \cos\delta \cos\omega + \sin\varphi \sin\delta) \quad (14)$$

Where, *I₀* = Solar constant, 1367 Wm⁻²; *n* = Day number, Jan 1 = 1; *φ* = Latitude; *δ* = Declination angle, and *ω* = Hour angle, 0 at solar noon.

We calculate the annual average TOA extraterrestrial solar power on a horizontal surface, *I_{TOA}*, for each latitude *φ* (location of a city or weather station) by calculating the average of *I_{TOA,I}* over 24 hours of the day and over all declination angles. In our calculations, we assume incoming and reflected atmospheric attenuation and scattering, *f*, is the same.

The global horizontal Insolation were extracted from weather data that included: station name, station WMO number, latitude, longitude, elevation in m, annual global horizontal insolation in kWh/m², and direct normal insolation in kWh/m². The annual insolation was calculated from these three "typical year" data sets: for the international locations (not US or Canada), ASHRAE (2012); for the US, NREL (2008); and for Canada, White Box Technologies (2014).

Procedure

1. We first calculated monthly averaged I_{TOA} for all latitude at one-degree interval from -90° to $+90^\circ$ and created a summary table. We checked our calculations by computing the average annual incoming solar radiation (weighted by degree latitude area) and comparing it with $1367/4 = 341.8 \text{ Wm}^{-2}$. The calculations were exact. Fig. 1a shows the calculated I_{TOA} for all latitudes. Fig. 1b shows the calculated area of the earth for each latitude angle with $\pm 0.5^\circ$. The average insolation on the earth was calculated by integrating values in Fig 1a as weighted by earth area with the same I_{TOA} (Fig. 1b) resulting in 341.8 Wm^{-2} .
2. For a given location (latitude φ), we then a) looked up for the I_{TOA} using Fig. 1a; b) calculates f_{avg} , using the annual GHI from local weather stations, (Eq 13); c) calculated the CO_2 offset (Eq. 11).

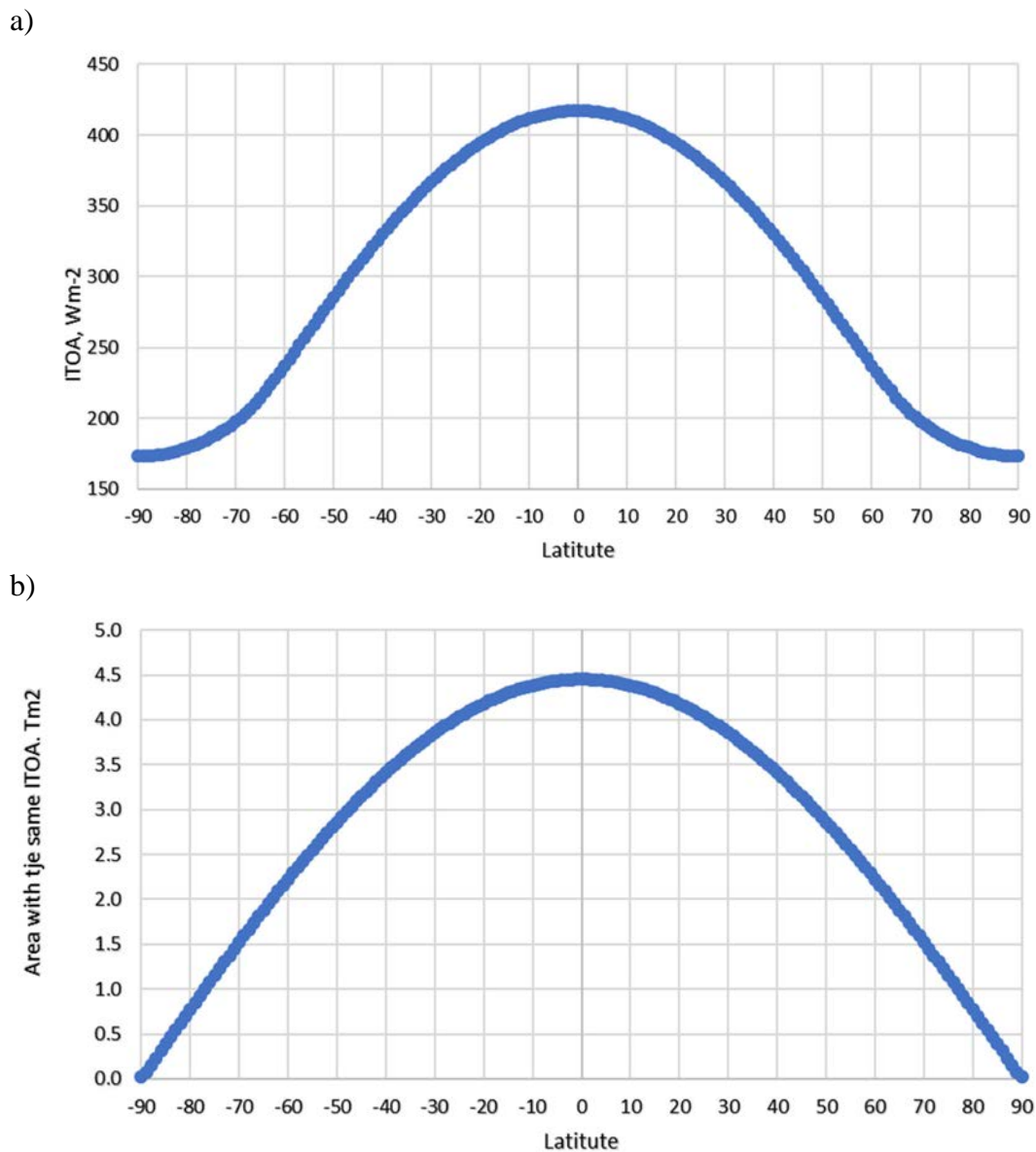


Figure 1. Calculated a) average annual horizontal TOA insolation and b) area of the Earth for a given latitude $\pm 0.5^\circ$, Tm^2 (10^{12} m^2)

Results and Discussions

Fig. 2 shows the measured GHI for all weather stations (data contains some apparent outliers). In extreme cases of very high and low latitudes, GHI is about 75 Wm^{-2} (about 40% of the extraterrestrial solar radiation of a horizontal surface). For latitudes -10° to 10° , GHI is about 200 Wm^{-2} (close to 48% of I_{TOA}). For latitudes -30° to -20° and 20° to 30° , GHI is the highest and approaches about 250 Wm^{-2} (about 70% of I_{TOA}).

The fraction of solar energy transmitted by the atmosphere, f is shown in Figure 3 and summarized in Table 1. The median atmospheric transmittance is about 49%. The maximum transmittance is about 79% for the Northern Hemisphere (desert land in northern Africa and Middle East) and for the Southern Hemisphere 69% in Kenya and 67% in South Africa.

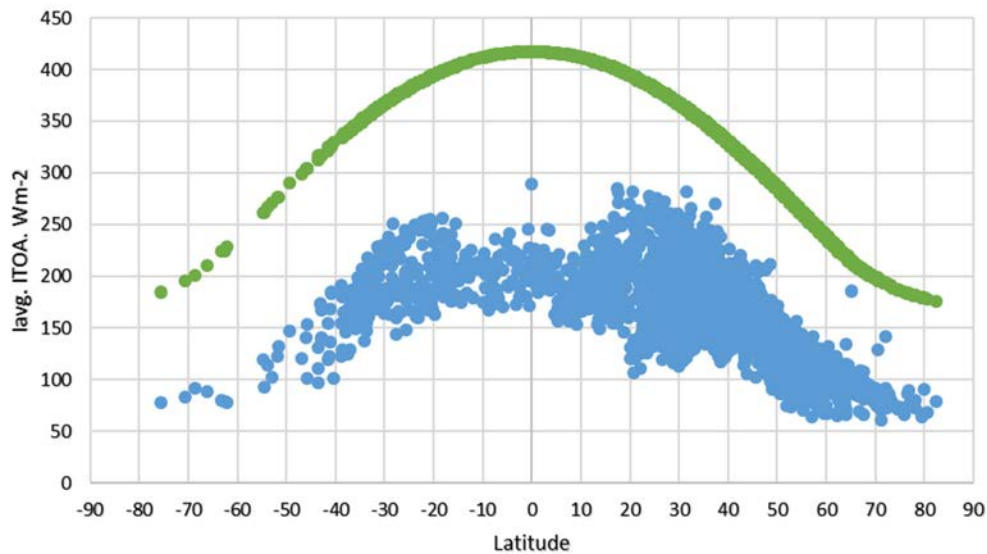


Figure 2. Top of Atmosphere and surface Global Horizontal Insolation, Wm^{-2} .

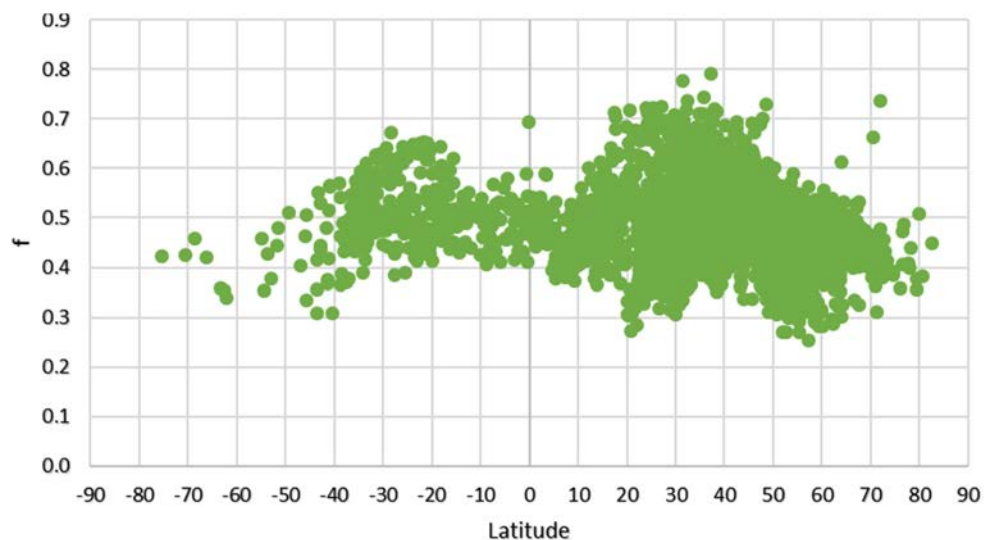


Figure 3. Atmospheric solar transmittance f . Note that f is around 0.5 around equator and it typically increases to a range of 0.65-0.75 around latitude $\pm 30^\circ$.

Table 1: Annual average solar energy transmittance through the atmosphere.

	Minimum	1 st Quartile	Median	3 rd quartile	Maximum
All locations	0.25	0.44	0.48	0.54	0.79
Northern Hemisphere	0.25	0.44	0.48	0.54	0.79
Southern Hemisphere	0.31	0.46	0.50	0.55	0.69

Kiehl and Trenberth (1997) estimate that of the total global average of 342 W m^{-2} incident shortwave solar radiation, 198 W m^{-2} ($f= 0.58$) is transmitted through the atmosphere and reaches the earth's surface. NASA's estimate of atmospheric solar transmittance is 0.55 (see Table 2). These estimates include both land and ocean surfaces. The amount of cloud cover on ocean surfaces is typically higher than land surfaces (King et al., 2013). Hence, in Kiehl and Trenberth calculations, the fraction of atmospheric transmittance over the land should be even higher than 0.55 or 0.58. This contrasts our calculated atmospheric solar transmittance of a median $f = 0.485$ for all weather stations around the world.

Table 2. Earth shortwave energy balance.

	Cloud and atmospheric reflectance	Atmospheric absorptance	Atmospheric transmittance	Surface reflectance
Kiehl and Trenberth 1997	0.225	0.195	0.58	0.09
NASA	0.225	0.225	0.55	0.07
Loeb et al 2021	0.226	0.227	0.547	0.087
This study, median			0.485	

Using Eq 11, we calculated the CO₂ offset for all weather stations. The results were then grouped and presented by countries and summarized by minimum, 25% quartile, median, 75% quartile, and maximum (see Table 3). The world-wide median CO₂ offset is about 1.8 kg. Akbari et al. (2009) estimate, based on Kiehl and Trenberth (1997) earth energy balance data, is 2.55 kg. The difference can almost entirely be explained by normalizing for the atmospheric transmittance of this study (0.485) and Kiehl and Trenberth (0.58).

The variation of CO₂ offset with atmospheric transmittance is shown in Figure 4. The CO₂ offset is highest where the atmospheric transmittance is greatest. As shown in Fig 3., atmospheric transmittance is highest around latitude 20° to 30° and -30° to -20°. The CO₂ offset is about 2-3 kg around the equator, 1.5-4 kg for -30° to -20° latitude and 1-5 kg for 20° - 30° latitude (see Fig. 5)

Table 3 CO₂ offset calculations are based on assumptions and simplifications used in Eq 11. The constant in Eq 11 is a linear function of current atmospheric CO₂ concentration. It is expected that the atmospheric CO₂ concentration to increase for at least the next few decades.

By using Eq 11 rather than hourly calculations (Eq 10), the overall reflected solar radiation is underestimated. The atmospheric transmittance (because of clouds) are typically lower during winter season (when the cloud cover is highest and the insolation is lowest). A limited analysis of this simplification showed that the CO₂ offset calculated by Eq 11 is about 10% lower than using the hourly calculations.

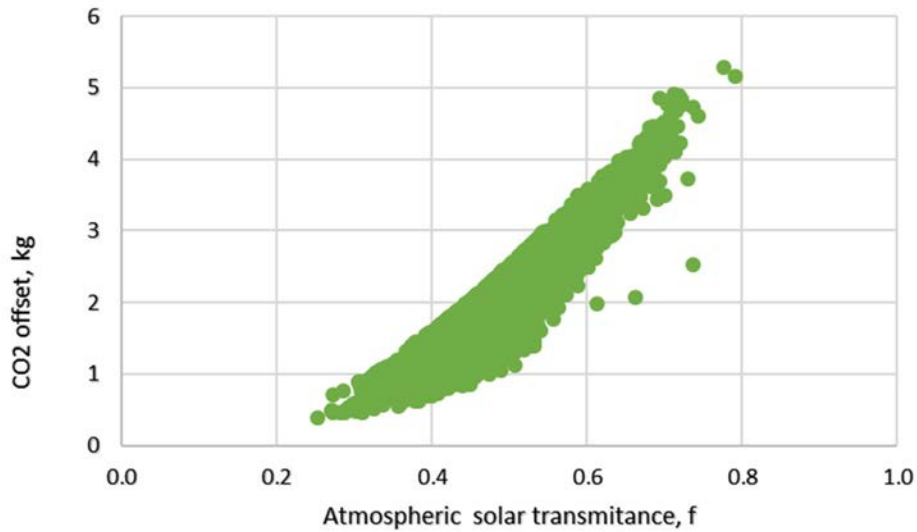


Figure 4. CO₂ offset as a function of atmospheric solar transmittance

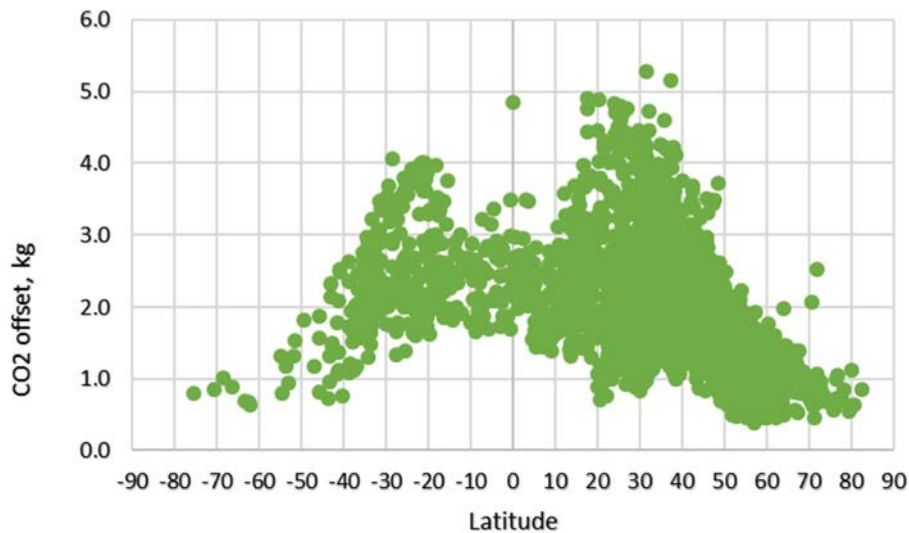


Figure 5. Variation of CO₂ offset with latitude.

The fraction of emitted CO₂ that stays in the atmosphere used in hour calculations is 0.50. Various studies show estimates of 0.45 to 0.55. This variation can introduce a $\pm 10\%$ variance in our estimated CO₂ offset.

The incoming GHI reported in the typical weather years is estimated to be accurate within $\pm 1\%$.

CO₂ offset based on RF and rise in global atmospheric temperature

The calculations of CO₂ based on the RF provide a current equivalency between CO₂ emissions and surface albedo modifications. Because of the Earth's inertia, the atmospheric temperature lags the RF changes by decades. Akbari et al (2012) used the simulations of Matthews et al (2012) that estimated that each 3700 Gt of emitted CO₂ results in a best guess of 1.75 K of global temperature change. Using this relationship, then the estimated CO₂ offset of increasing albedo of 1 m² of surface calculated at about 7 kg. On the other hand, Valone (2021) provides a simple correlation that each 20 ppm increase in atmospheric CO₂ concentration results in 1K temperature rise of the globe. Based on this correlation and the

correlation from Akbari et al (2012) that changing surface albedo by 0.01 of a m² of surface results in 3.2x10⁻¹⁵ K global temperature change, we estimate a CO₂ offset of 1 kg. Literature is saturated with models that estimate the temperature rise with increasing CO₂ emissions. Our CO₂ offset estimate of world average 2 kg for increasing albedo of a m² of surface by 0.01 falls within in the range of 1-7 kg from the two studies mentioned above.

Conclusions

We introduced a simplified technique to calculate a CO₂-equivalency (offset) for changes in the albedo of land surfaces areas on top of the atmosphere RF. Calculations were carried out for about 4400 weather stations world-wide. The calculated world-wide median CO₂ offset was about 2 kg per 0.01 albedo change of a m² of a surface. The CO₂ offset is highest where the atmospheric transmittance is high, around latitude 20° to 30° and -30° to -20°. The CO₂ offset is about 2 - 3 kg around the equator, 1.5 - 4 kg for -30° to -20° latitude and 1 - 5 kg for 20° to 30° latitude. This simplified method allows countries to develop policies monetizing the effect of high-albedo urban surface to counter global warming.

Table 3. CO₂ offset (kg) by increasing albedo of a m² of a surface by 0.01. The CO₂ offset in the highest in countries with minimal cloud cover, typically around 20° to 30°. The world median offset is about 1.8 kg.

Country	Minimum	1st Quartile	Median	3rd Quartile	Maximum
Antigua and Barbuda	2.8	2.8	2.8	2.8	2.8
United Arab Emirates	4.0	4.0	4.1	4.3	4.4
Argentina	1.2	2.0	2.2	2.4	3.5
Armenia	2.5	2.5	2.5	2.5	2.5
American Samoa	1.8	1.8	1.8	1.8	1.8
Antarctica	0.6	0.7	0.8	0.9	1.0
Antigua and Barbuda	2.5	2.5	2.5	2.5	2.5
Australia	0.7	2.0	2.6	3.4	4.0
Austria	1.2	1.4	1.6	1.9	2.2
Azerbaijan	1.9	2.0	2.0	2.0	2.1
Belgium	0.9	1.0	1.1	1.1	1.3
Benin	1.5	1.7	1.8	2.0	2.1
Burkina Faso	2.3	2.3	2.3	2.3	2.4
Bulgaria	1.7	1.8	1.9	2.1	2.8
Bahrain	2.3	2.3	2.3	2.3	2.3
Bahamas	2.5	2.5	2.5	2.5	2.5
Bosnia and Herzegovina	1.6	1.6	1.7	1.9	2.2
Belarus	1.2	1.4	1.4	1.5	1.6
Belize	1.8	1.8	1.8	1.8	1.8
Bolivia	2.1	2.1	2.5	3.0	3.4
Brazil	1.4	1.9	2.2	2.5	2.9
Barbados	2.1	2.1	2.1	2.1	2.1
Brunei	2.2	2.2	2.2	2.2	2.2
Botswana	2.9	2.9	2.9	3.1	3.3
Cocos Island	2.1	2.6	2.6	2.6	2.6
Switzerland	1.1	1.4	1.6	2.1	2.5
Chile	0.9	1.6	2.1	2.7	3.2
China	0.8	1.5	2.0	2.4	3.9

Country	Minimum	1st Quartile	Median	3rd Quartile	Maximum
Cote D'ivoire	1.7	1.7	1.7	1.7	1.7
Cook Islands	2.0	2.0	2.0	2.0	2.0
Colombia	1.6	1.7	2.4	2.7	3.5
Cabo Verde	2.7	2.7	2.7	2.7	2.7
Costa Rica	2.1	2.1	2.1	2.1	2.1
Cuba	2.5	2.5	2.5	2.5	2.5
Cyprus	2.5	2.5	2.5	2.6	2.6
Czechia	1.1	1.2	1.3	1.4	2.3
Germany	0.8	1.0	1.1	1.2	1.7
Denmark	0.6	0.8	1.0	1.0	1.1
Dominican Republic	2.5	2.5	2.6	2.6	2.7
Algeria	2.2	2.6	2.9	3.9	4.4
Egypt	3.1	3.6	4.2	4.5	4.8
Western Sahara	3.5	3.5	3.5	3.5	3.5
Spain	1.0	2.0	2.3	2.6	3.0
Estonia	1.2	1.3	1.3	1.3	1.3
Finland	1.0	1.1	1.2	1.3	1.5
Fiji	2.0	2.0	2.0	2.0	2.0
Falkland Island	1.3	1.3	1.3	1.3	1.3
France	0.8	1.1	1.3	1.7	3.1
Faroe Island	0.5	0.5	0.5	0.5	0.5
Micronesia	1.4	1.4	1.5	1.6	1.8
Great Britain	0.5	0.7	0.8	1.0	1.2
Georgia	2.0	2.0	2.0	2.0	2.0
Guernsey	0.8	0.8	0.8	0.8	0.8
Gibraltar	2.2	2.2	2.2	2.2	2.2
Greece	2.1	2.3	2.3	2.4	2.6
Grenada	2.5	2.5	2.5	2.5	2.5
Greenland	1.0	1.1	1.1	1.4	1.4
French Guiana	2.6	2.6	2.6	2.6	2.6
Guam	1.8	2.0	2.1	2.3	2.4
Honduras	1.8	1.9	2.0	2.3	2.5
Hungary	1.3	1.5	1.5	1.6	1.9
Indonesia	1.7	2.1	2.5	2.7	3.5
Isle of Man	0.7	0.7	0.7	0.7	0.7
India	1.6	2.5	2.8	3.1	3.7
British Indian Ocean	1.8	1.8	1.8	1.8	1.8
Ireland	0.6	0.7	0.7	0.7	0.8
Iran	1.7	2.8	3.1	3.5	4.3
Iceland	0.5	0.6	0.9	0.9	1.0
Israel	2.5	2.6	3.1	4.0	4.3
Italy	1.5	1.9	2.1	2.2	2.5
Jamaica	2.8	2.8	2.8	2.9	2.9
Jersey	0.9	0.9	0.9	0.9	0.9
Jordan	2.8	3.6	3.9	3.9	4.2

Country	Minimum	1st Quartile	Median	3rd Quartile	Maximum
Japan	1.1	1.3	1.5	1.6	2.0
Kazakhstan	1.4	1.8	1.9	2.2	2.7
Kenya	2.2	2.5	2.7	2.9	4.9
Kyrgyzstan	2.1	2.3	2.5	2.6	2.8
Kiribati	2.6	2.6	2.6	2.6	2.6
Korea, South	1.5	1.7	1.8	1.9	2.1
Kuwait	2.6	2.6	2.6	2.6	2.6
Lebanon	2.4	2.4	2.4	2.4	2.4
Libya	3.0	3.1	3.4	4.1	4.7
Lithuania	0.9	1.3	1.3	1.4	1.4
Luxembourg	1.2	1.2	1.2	1.2	1.2
Latvia	1.1	1.2	1.3	1.3	1.4
Macao	1.0	1.0	1.0	1.0	1.0
Morocco	2.1	2.4	2.7	3.0	3.8
Moldova	1.6	1.6	1.6	1.6	1.6
Madagascar	2.2	2.3	2.5	2.8	3.1
Mexico	1.9	2.5	2.7	3.0	3.5
Marshall Islands	1.6	1.6	1.6	1.6	1.6
North Macedonia	2.1	2.1	2.2	2.2	2.2
Mali	2.3	2.8	3.3	3.5	3.7
Malta	2.3	2.3	2.3	2.3	2.3
Myanmar	1.9	1.9	1.9	1.9	1.9
Montenegro	2.1	2.1	2.1	2.2	2.2
Mongolia	1.8	2.1	2.2	2.4	2.6
Northern Mariana Islands	1.7	1.8	1.8	1.8	1.9
Mozambique	2.6	2.6	2.6	2.6	2.6
Mauritania	3.7	3.7	3.8	3.8	3.8
Martinique	2.8	2.8	2.8	2.8	2.8
Mauritius	1.7	1.9	2.2	2.5	2.6
Malaysia	1.8	2.1	2.1	2.2	2.6
Mayotte	2.7	2.7	2.7	2.7	2.7
Namibia	3.0	3.3	3.4	3.5	3.8
New Caledonia	2.1	2.1	2.2	2.5	2.8
Niger	2.3	2.6	2.7	2.9	3.7
Norfolk Island	1.8	1.8	1.8	1.8	1.8
Netherlands	0.8	0.9	0.9	1.0	1.1
Norway	0.5	0.7	0.8	1.0	1.6
New Zealand	0.8	1.0	1.1	1.2	1.3
Oman	2.8	3.4	3.6	3.9	4.8
Pakistan	2.7	2.8	3.0	3.1	3.2
Peru	1.8	2.3	2.8	3.1	3.5
Philippines	1.4	1.7	1.8	2.2	2.8
Palau	1.6	1.6	1.6	1.6	1.6
Poland	0.9	1.1	1.2	1.5	1.9
Puerto Rico	2.1	2.1	2.2	2.2	2.5
Korea, North	1.0	1.2	1.3	2.0	2.3

Country	Minimum	1st Quartile	Median	3rd Quartile	Maximum
Portugal	1.0	1.8	2.0	2.2	2.6
Paraguay	2.1	2.3	2.3	2.4	2.7
French Polynesia	1.3	1.8	2.2	2.6	2.9
Qatar	2.5	2.5	2.5	2.5	2.5
Reunion	2.7	2.7	2.7	2.7	2.7
Romania	1.4	1.6	1.7	1.8	2.2
Russia	0.6	1.2	1.4	1.6	2.4
Saudi Arabia	2.6	4.1	4.3	4.4	4.9
Senegal	2.7	2.8	3.2	3.2	4.0
Singapore	2.0	2.0	2.0	2.0	2.0
Saint Helena	2.5	2.5	2.5	2.5	2.5
Svalbard and Jan Mayen	0.7	0.7	0.7	0.8	0.8
Solomon Islands	2.4	2.4	2.4	2.4	2.4
Saint Pierre and Miquelon	1.4	1.4	1.4	1.4	1.4
Serbia	1.4	1.7	1.8	1.9	2.2
Slovakia	1.5	1.7	1.7	1.8	2.5
Slovenia	1.6	1.6	1.6	1.7	1.8
Sweden	0.9	1.0	1.1	1.3	1.5
Seychelles	2.1	2.1	2.1	2.1	2.1
Syria	2.3	2.7	2.9	3.6	4.0
Chad	3.6	3.6	3.6	3.6	3.6
Togo	1.9	1.9	1.9	1.9	1.9
Thailand	1.7	1.9	2.4	2.6	2.7
Tajikistan	3.0	3.0	3.0	3.0	3.0
Turkmenistan	2.5	2.7	3.0	3.1	3.2
Tonga	1.6	1.8	1.9	2.0	2.2
Trinidad and Tobago	2.0	2.0	2.0	2.0	2.0
Tunisia	2.3	2.4	3.0	3.2	3.6
Turkey	1.3	2.2	2.5	2.6	2.9
Taiwan	0.8	1.3	1.5	1.8	2.3
Tanzania	2.5	2.5	2.5	2.5	2.5
Ukraine	1.3	1.5	1.6	1.7	1.9
Uruguay	1.8	1.9	2.0	2.1	2.2
Uzbekistan	2.2	2.4	2.8	2.9	3.1
Venezuela	1.7	1.9	2.1	2.1	2.1
Viet Nam	0.7	1.0	1.4	1.6	2.6
Vanuatu	1.9	2.0	2.1	2.2	2.2
Wallis and Futuna	2.0	2.0	2.0	2.0	2.0
South Africa	0.8	2.0	2.5	3.2	4.1
Zimbabwe	2.3	2.4	2.6	2.8	3.3
United States	0.4	1.7	2.0	2.5	5.3
Canada	0.6	1.1	1.4	1.5	2.5
All Countries	0.4	1.4	1.8	2.4	5.3

Acknowledgements

Funding for this research was provided by the Natural Sciences and Engineering Research Council of Canada under the discovery program. This research was in part funded by: Juan Carlos Pereira, President of Instituto Provincial de Desarrollo Habitacional (IPRODHA) - (Provincial Institute of Housing Development), Gervasio Malagrida, Minister of Climate Change, Province of Misiones Argentina, and MACOMA Environmental Technologies, Corp. Nevada, USA.

References

- Akbari, H., H.D. Matthews, and D. Seto. 2012. "The long-term effect of increasing the albedo of urban areas," *Environ. Res. Lett.* 7, 024004 (10pp).
- Akbari, H., S. Menon, and A. Rosenfeld. 2009. "Global Cooling: Increasing World-wide Urban Albedos to Offset CO₂," *Climatic Change*, 95 (3-4).
- Akbari, H., S. Konopacki, and M. Pomerantz. 1999. "Cooling energy savings potential of reflective roofs for residential and commercial buildings in the United States," *Energy*, **24**: 391-407.
- ASHRAE 2012. "International Weather for Energy Calculations Version 2" (IWEC2), American Society of Heating, Refrigerating, and Air-Conditioning Engineers, Atlanta GA. technical report: Huang, Y.J. 2011. "ASHRAE Research Project 1477-RP (Development of 3,012 typical year weather files for international locations)", Final Report, ASHRAE, Atlanta Ga.
- Hosseini, M. and H. Akbari. 2016. "Effect of cool roofs on commercial buildings energy use in cold climates." *Energy and Buildings*, **114**, 143-155.
- IPCC 2014. Lucon O., D. Ürge-Vorsatz, A. Zain Ahmed, H. Akbari, et al (eds.). Cambridge University Press, Cambridge, United Kingdom and New York, NY, USA. Chap 9, p699.
- Jandaghian, Z. and H. Akbari. 2021. "Increasing urban albedo to reduce heat-related mortality in Toronto and Montreal, Canada." *Energy & Buildings* 237.
- Loeb, Norman G.; Johnson, Gregory C.; Thorsen, Tyler J.; Lyman, John M.; et al. 2021. "[Satellite and Ocean Data Reveal Marked Increase in Earth's Heating Rate](#)". *Geophysical Research Letters*. **48**(13), 15 June.
- Kiehl JT, Trenberth KE. 1997. "Earth's annual global mean energy budget." *Bull Am Meteorol Soc*78(2):197-208, February.
- King, DM, S Platnick, WP Menzel, SA Ackerman, and PA Hubanks. 2013. Spatial and Temporal Distribution of Clouds Observed by MODIS Onboard the Terra and Aqua Satellites. *IEEE Transactions on Geoscience and Remote Sensing*, Vol. 51, NO. 7, July.
- Myhre G, EJ. Highwood, KP Shine, F Stordal. 1998. "New estimates of radiative forcing due to well mixed greenhouse gases." *Geophysical Research Letters*, **25** (14), 2715-2718, July 15.
- NOAA 2022. "[Carbon dioxide now more than 50% higher than pre-industrial levels | National Oceanic and Atmospheric Administration](#)". *www.noaa.gov*. Retrieved 14 June.
- TMY3 data for 1,020 US locations, National Renewable Energy Laboratory, Golden CO. technical report: Wilcox, S. and Marion, W. 2008. User's Manual for TMY3 Data Sets, NREL/TP-581-43156, National Renewable Energy Laboratory, Golden CO.
- Valone, T. F. 2021. "Linear Global Temperature Correlation to Carbon Dioxide Level, Sea Level, and Innovative Solutions to a Projected 6°C Warming by 2100." *Journal of Geoscience and Environment Protection*, 9, 84-135.
- Vaughan, N.E., Lenton, T.M. 2011. A review of climate geoengineering proposals. *Climatic Change* **109**, 745-790.